

## Spectroscopy of 3, 4, 9, 10-perylenetetracarboxylic dianhydride (PTCDA) attached to rare gas samples: Clusters vs. bulk matrices. I. Absorption spectroscopy

Matthieu Dvorak, Markus Müller, Tobias Knoblauch, Oliver Bünermann, Alexandre Rydlo et al.

Citation: *J. Chem. Phys.* **137**, 164301 (2012); doi: 10.1063/1.4759443

View online: <http://dx.doi.org/10.1063/1.4759443>

View Table of Contents: <http://jcp.aip.org/resource/1/JCPSA6/v137/i16>

Published by the [American Institute of Physics](#).

---

### Additional information on *J. Chem. Phys.*

Journal Homepage: <http://jcp.aip.org/>

Journal Information: [http://jcp.aip.org/about/about\\_the\\_journal](http://jcp.aip.org/about/about_the_journal)

Top downloads: [http://jcp.aip.org/features/most\\_downloaded](http://jcp.aip.org/features/most_downloaded)

Information for Authors: <http://jcp.aip.org/authors>

## ADVERTISEMENT



**ALL THE PHYSICS  
OUTSIDE OF  
YOUR JOURNALS.**

www.physics today.org  
**physics  
today**

# Spectroscopy of 3, 4, 9, 10-perylenetetracarboxylic dianhydride (PTCDA) attached to rare gas samples: Clusters vs. bulk matrices.

## I. Absorption spectroscopy

Matthieu Dvorak,<sup>1</sup> Markus Müller,<sup>1</sup> Tobias Knoblauch,<sup>2</sup> Oliver Bünermann,<sup>1,3</sup> Alexandre Rydlo,<sup>4</sup> Stefan Minniberger,<sup>4</sup> Wolfgang Harbich,<sup>4</sup> and Frank Stienkemeier<sup>1</sup>

<sup>1</sup>Physikalisches Institut, Universität Freiburg, Hermann-Herder-Str. 3, 79104 Freiburg, Germany

<sup>2</sup>I. Physikalisches Institut, Universität Stuttgart, Pfaffenwaldring 57, 70550 Stuttgart, Germany

<sup>3</sup>Institut für Physikalische Chemie, Georg-August-Universität, Tammannstr. 6, 37077 Göttingen, Germany

<sup>4</sup>Institut de Physique des Nanostructures, École Polytechnique Fédérale de Lausanne (EPFL), CH-1015 Lausanne, Switzerland

(Received 10 June 2012; accepted 1 October 2012; published online 22 October 2012)

The interaction between 3, 4, 9, 10-perylenetetracarboxylic dianhydride (PTCDA) and rare gas or para-hydrogen samples is studied by means of laser-induced fluorescence excitation spectroscopy. The comparison between spectra of PTCDA embedded in a neon matrix and spectra attached to large neon clusters shows that these large organic molecules reside on the surface of the clusters when doped by the pick-up technique. PTCDA molecules can adopt different conformations when attached to argon, neon, and para-hydrogen clusters which implies that the surface of such clusters has a well-defined structure without liquid or fluxional properties. Moreover, a precise analysis of the doping process of these clusters reveals that the mobility of large molecules on the cluster surface is quenched, preventing agglomeration and complex formation. © 2012 American Institute of Physics. [<http://dx.doi.org/10.1063/1.4759443>]

## I. INTRODUCTION

The structure of rare gas aggregates has been subject to controversial discussions since the early developments of cluster physics. Large argon clusters do not form the expected hexagonal close-packed (hcp) crystal structure; instead a face-centered cubic (fcc) or mixed closed packed structures is preferred.<sup>1</sup> In spite of the huge improvements in spectroscopic techniques during the last few decades, fundamental characteristics still remain unclear: no accordance has been found on the cluster size above which the lattice structure changes from fcc to hcp.<sup>2,3</sup> Moreover, small clusters have been assigned to liquid-like behavior<sup>4-6</sup> and the cluster size above which these clusters solidify is not yet well-characterized. The study of the above mentioned characteristics is limited by the transparency of rare gas clusters in the visible range, limiting the use of many standard spectroscopic methods. To circumvent this problem, rare gas clusters are doped with a chromophore (atom or molecule). Studying the spectral response of this chromophore as a function of the cluster parameters allows one to gain insights into the cluster characteristics. This concept has already been developed in 1980s<sup>7</sup> and applied successfully since then (see for example Refs. 8–10), being nowadays a common method.

Among the different cluster characteristics studied, conclusive information could be obtained on the cluster phase state and phase transition as a function of size. Benzene-doped argon clusters show a liquid-solid transition at a cluster size of  $N = 21$ .<sup>4</sup> For xenon-doped neon clusters, this transition lies at  $N = 300$ .<sup>6</sup> To our knowledge no such studies have been performed involving large doped hydrogen clusters. Large neat hydrogen clusters obtained by supersonic ex-

pansion have a temperature of 4.2 to 4.5 K.<sup>11</sup> For smaller clusters, Monte-Carlo simulation postulated a superfluid phase for clusters sizes less than 26 molecules and for temperatures below 1.5 K.<sup>12</sup> These numbers have been obtained for para-hydrogen which correspond to molecules with their two proton spins forming a singlet state. Experiments on large hydrogen clusters involving Raman spectroscopy revealed a solid structure when formed in a supersonic expansion.<sup>13</sup> Only the co-expansion of helium and hydrogen with less than 1% hydrogen<sup>13</sup> or the aggregation mechanism of somewhat smaller hydrogen clusters in helium droplets have shown liquid-like properties.<sup>14,15</sup>

Large rare gas clusters have been shown to provide an ideal support for chemical reactions and catalysis due to the confinement of the reactants to the clusters' surface and the corresponding high reaction probabilities.<sup>16</sup> Correspondingly, single atoms as well as di- and tri-atomic molecules and a few larger molecules (e.g., SiF<sub>4</sub>, SF<sub>6</sub>) have been attached to large argon clusters.<sup>17-20</sup>

Historically, the study of doped rare gas matrices was motivated by astrochemistry studies. Indeed, perylene derivatives as well as other large polycyclic aromatic hydrocarbons (PAH) have long been postulated to compose a non-negligible part of interstellar matter<sup>21</sup> and to partly explain the presence of absorption features in the visible spectral region, the so-called diffuse interstellar bands (DIB).<sup>22</sup> The study of such molecules in a weakly interacting medium at low temperatures should ascertain these postulates.

Determining important clusters' properties, several more detailed questions remain: Is the cluster surface also solid? If one dopes these clusters after their formation, can one expect that the chromophores remain at the clusters' surface or

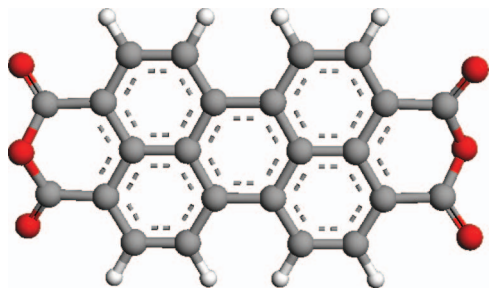


FIG. 1. The PTCDA molecule (3, 4, 9, 10-perylenetetracarboxylic dianhydride,  $C_{24}H_8O_6$ ) is composed of a perylene core and two anhydride end groups.

can the deposited energy induce surface melting which would allow the chromophore to immerse? Provided that the chromophores remain on the clusters' surface, how is the surface mobility? In the case of multiple doping, can these chromophores aggregate and form complexes? The present work answers these questions for argon, neon, and para-hydrogen clusters. We compare spectroscopic results of 3, 4, 9, 10-perylenetetracarboxylic dianhydride (PTCDA) chromophores attached to large rare gas and hydrogen clusters with measurement on PTCDA embedded in rare gas matrices for which the inside localization and the solid structure are well established.

PTCDA ( $C_{24}H_8O_6$ , see Fig. 1) is a perylene derivative which has been studied already for various systems. For example, deposited on surfaces for graphene,<sup>23</sup> muscovite mica(0001), and Au(111),<sup>24</sup> this planar molecule can self-assemble into well-defined orientations.<sup>25</sup> A herringbone structure is preferred in multilayer films or bulk crystals.  $\pi$ -stacking of PTCDA molecules leads to semi-conducting properties of the organic layers.<sup>26–28</sup> These self-assembly and semi-conducting properties are much desired for the development of efficient electro-optical devices.<sup>29–31</sup> Therefore, PTCDA is not only studied for a fundamental understanding of organic semiconducting properties but because it is also found in device assemblies.

As far as bulk matrix isolated studies are concerned, among the many measurements obtained for ions and smaller molecules (see a list of them in Ref. 32), a few studies were made on larger PAHs and their ions embedded in argon and/or in neon matrices:  $C_{60}$ ,<sup>33</sup> naphthalene,<sup>34</sup> phenanthrene,<sup>35</sup> pentacene,<sup>36</sup> 9,10-dichloroanthracene,<sup>37</sup> benzo[g,h,i]perylene,<sup>38</sup> and perylene.<sup>39,40</sup> For PTCDA, however, only measurement in  $SiO_2$  matrices are known to us.<sup>41</sup>

The present article is structured as follows: first, absorption measurements of PTCDA molecules embedded in a neon matrix are presented. In Sec. II, PTCDA molecules are attached to large neon, argon, and para-hydrogen clusters. Comparison between matrix and clusters measurements allow decisive conclusions on the site occupation of the attached PTCDA molecules. Finally, a careful analysis of the shape of the observed optical features as well as their dependency on external parameters allow to draw conclusions on the conformation and the mobility of PTCDA molecules on such clusters.

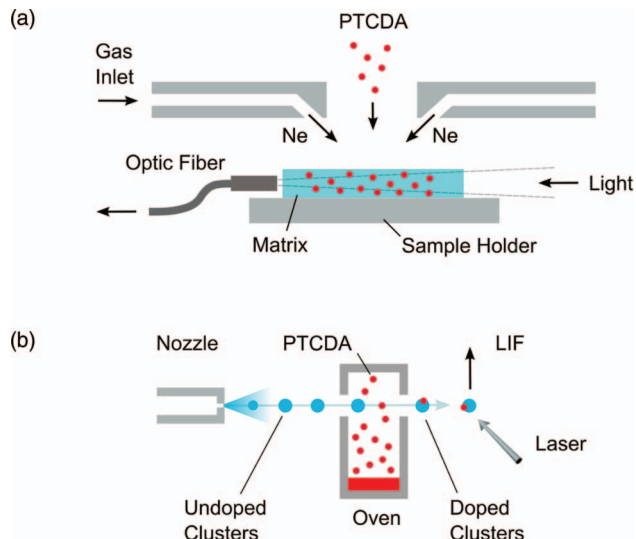


FIG. 2. Experimental setup for the matrix deposition (a) and the cluster beam spectroscopy (b).

Our related results on fluorescence emission spectroscopy of the same systems (referred to as Paper II) are published in a separate publication.<sup>42</sup>

## II. EXPERIMENTAL SETUP

PTCDA-doped neon matrices are produced by co-deposition of neon and PTCDA on an aluminum mirror cooled by a pulse tube cryocooler (SRP-052A Cryocooler, Sumitomo Heavy Industries), see Fig. 2(a). An effusive beam of PTCDA molecules is emitted by an oven placed about 30 cm away from the sample holder. The PTCDA flux is controlled by the oven temperature. Neon gas, purified by cryotrapping is co-deposited at a ratio of about  $5 \times 10^4$ : 1 with PTCDA. A standard 100 W quartz tungsten halogen lamp (QTH) and a deuterium lamp (Hamamatsu L7296) cover the optical range from 10 000 to 50 000  $cm^{-1}$ . The light is focused on a narrow slit on the side of the 50  $\mu m$  thick matrix which is used as a light guide.<sup>43</sup> After crossing the PTCDA-rare gas matrix, the transmitted light is collected by an optical fiber (Ocean Optics Inc. 400-SR, core diameter: 400  $\mu m$ ) coupled to a spectrograph (Jobin-Yvon T64000) equipped with a liquid nitrogen cooled CCD detector (Spectrum One). The total useful transmission range strongly depends on the matrix quality and in the case of Ne ranges from 8000 to 45 000  $cm^{-1}$ . Absorption is expressed as  $\log(I_0/I)$  where  $I_0$  is always obtained from a reference spectrum of a pure matrix grown under identical conditions. Typical absorbances are 0.05–0.1. Further details on this setup and the applied method can be found in Ref. 43.

For cluster beam spectroscopy, large argon, neon, and para-hydrogen clusters as well as helium droplets are produced via the expansion of highly pressurized gas through a nozzle, see Fig. 2(b). For argon and para-hydrogen clusters, a 10  $\mu m$  nozzle is used (continuous beam); for neon clusters and helium droplets a pulsed nozzle has been used (Even-Lavie valve, 60  $\mu m$  trumpet nozzle, operated at 500 Hz repetition rate).

Normal hydrogen has a natural para/ortho relative concentration of about 25%/75% at standard temperature and pressure. We employ an online catalytic converter to transform ortho- $\text{H}_2$  into para- $\text{H}_2$ : before entering the cluster source the hydrogen gas passes through a small container cooled down to 15 K and filled with a catalyst (here  $\text{Al}_2\text{O}_3$  powder).<sup>44</sup> In this way nearly all the ortho- $\text{H}_2$  is converted into para- $\text{H}_2$  (at 20 K and thermal equilibrium already 99.8% of the molecules are in the para state<sup>45</sup>).

The mean size of rare gas and para-hydrogen clusters depends on the expansion parameters and can be estimated with the help of scaling laws<sup>46</sup> and measured values of argon,<sup>47,48</sup> neon,<sup>48</sup> and para-hydrogen clusters.<sup>49,50</sup> With the expansion parameters used for argon (90 bars, 300 K), the clusters have a mean size of about 450 atoms. Neon clusters (85 bar, 90 K) consist of about 6000 atoms and para-hydrogen clusters (20 bar, 43 K) have a mean size of roughly 14 000 molecules.

For clusters formed in a supersonic expansion, the cluster sizes follow log-normal distributions. For argon clusters and helium droplets, such distributions have been characterized and it was shown that the FWHM of the size distribution is almost equal to their mean size.<sup>51</sup> For argon clusters containing more than 800 atoms a temperature of  $37 \text{ K} \pm 5 \text{ K}$  has been determined; at a cluster size of 150, a temperature of  $34 \text{ K} \pm 3 \text{ K}$  has been found.<sup>52</sup> In the present study, the temperature of argon clusters is expected to be similar. Neon clusters produced in the present study are expected to have a temperature of  $10 \text{ K} \pm 4 \text{ K}$ .<sup>52</sup>

Helium nanodroplets produced via supersonic expansion (60 bar, 20 K, mean size: 20 000 atoms) are used as reference because their properties are well known.<sup>53</sup> The dopants — with the exception of alkaline and some alkaline earth atoms — are known to be located at the center of helium droplets and thermalize with the droplets temperature (0.37 K).<sup>53</sup> This low temperature leads to a great simplification of vibronic spectra as only the lowest vibrational level of the electronic ground state is populated. Moreover, the weak interaction with the surrounding helium leads to only minor perturbations and narrow lines. Excitation spectra of PTCDA molecules embed-

ded in helium droplets have been extensively discussed in Ref. 54.

After formation, the clusters are doped by means of the pickup technique in a heated oven cell (length 12 mm) containing PTCDA powder (Sigma Aldrich, used without further purification). By varying the PTCDA partial pressure the mean number of PTCDA molecules picked-up can be changed. The effective partial pressure  $\bar{P}$  has been calculated from the kinetic vapor pressure formula and the measured oven temperature  $T_{\text{oven}}$ :

$$\bar{P} = aT_{\text{oven}}^{3/2} \exp(-b/T_{\text{oven}}).$$

The parameters  $a = 1000 \text{ K}^{-3/2} \text{ mbar}$  and  $b = 15\,100 \text{ K}$  were determined from best fits to monomer pick-up dependencies.<sup>55</sup>

In a separate vacuum chamber the cluster beam intersects the laser beam used for spectroscopy. The fluorescence light is imaged onto a photomultiplier (Hamamatsu R5600-U-01) by a set of lenses, the optical axes of which lies perpendicularly to both the laser and the cluster beam. A second photomultiplier monitors background photons (laser stray light and LIF of PTCDA molecules ejected effusively from the oven, i.e., molecules not attached to a cluster). The laser system used for the cluster measurements consists of a pulsed dye laser (Sirah Cobra, Coumarin 102) pumped by a Nd:YAG laser (Edge-wave IS-IIIIE) at a repetition rate of 1 kHz with pulse lengths of about 10 ns. The dye laser system has a maximal energy of about  $100 \mu\text{J}$  per pulse but was attenuated to about  $1 \mu\text{J}$  per pulse in order to suppress saturation effects.

### III. RESULTS

#### A. PTCDA embedded in neon matrix

Absorption spectra of PTCDA embedded in neon matrices have been recorded with the QTH and  $\text{D}_2$  lamps as shown in Fig. 3. The spectra are characterized by four broad bands (FWHM  $500\text{--}700 \text{ cm}^{-1}$ ) containing sub-structures. However, when comparing the two spectra, some discrepancies are

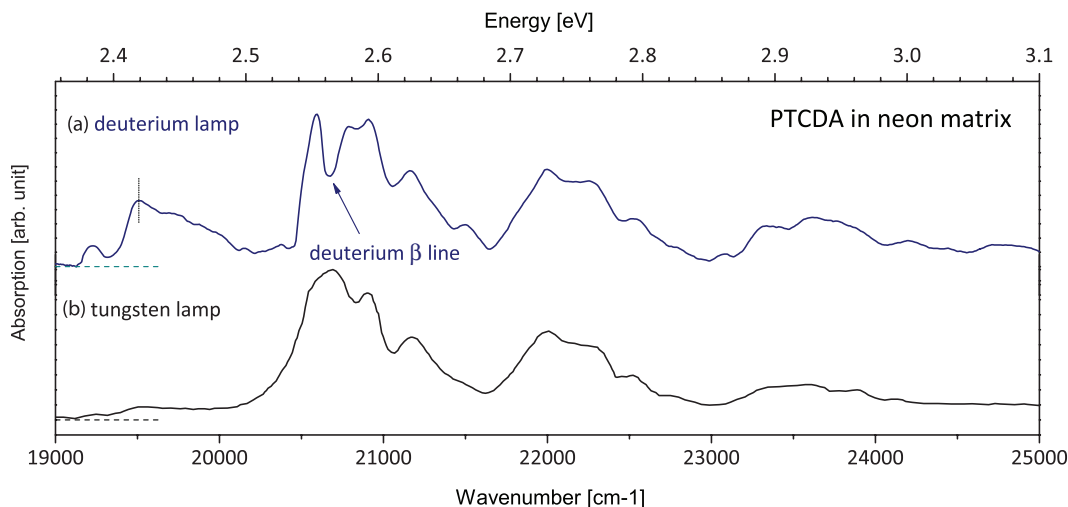


FIG. 3. Absorption spectra of PTCDA in a neon matrix excited with a deuterium lamp (a) and a tungsten lamp (b). In (a), the peak at around  $19\,500 \text{ cm}^{-1}$  is attributed to charged PTCDA molecules and the depletion at around  $20\,600 \text{ cm}^{-1}$  is a side effect of the presence of the Balmer line  $D\beta$  at this wavenumber.

observed which result from peculiar distributions of emission frequencies of these lamps. The tungsten lamp has an emission spectrum limited to the visible range (roughly between  $12\,500\text{ cm}^{-1}$  and  $25\,000\text{ cm}^{-1}$ ), whereas the deuterium lamp emits further into the UV/VUV (the continuous part of the spectrum extends to about  $55\,000\text{ cm}^{-1}$ ). The VUV contribution of the  $\text{D}_2$  lamp has direct implications on the absorption spectra of the PTCDA-doped matrix. The spectrum (Fig. 3(a)) shows an additional band at about  $19\,500\text{ cm}^{-1}$ , which is hardly observable in the spectrum measured with the tungsten lamp (Fig. 3(b)). We assign this peak to PTCDA cations. The first ionization threshold of PTCDA is between  $50\,000\text{ cm}^{-1}$  and  $55\,000\text{ cm}^{-1}$ ,<sup>56–58</sup> which can be accessed in a 1-photon process with the  $\text{D}_2$  lamp but not with the QTH lamp. This interpretation is corroborated by different studies on neutral and charged PAH molecules embedded in rare gas matrices showing that PAH ions absorb in the visible-near IR domain, with typical redshifts of some hundreds or some thousands of wavenumbers compared to the absorption bands of the neutral molecules.<sup>22</sup> According to our measured spectra the ions absorb about  $1200\text{ cm}^{-1}$  redshifted, a value which is close to previous measurements on similar molecules. For example, for pentacene in neon a redshift of about  $1200\text{ cm}^{-1}$  has been observed of the absorption bands of cations compared to neutral molecules.<sup>36</sup> For perylene, similar redshifts have been observed for anions ( $\sim 900\text{ cm}^{-1}$ ) and for cations ( $\sim 1700\text{ cm}^{-1}$ ).<sup>59</sup> The second obvious difference of both spectra is the pronounced dip at  $\sim 20\,600\text{ cm}^{-1}$  which is related to the  $\beta$  Balmer line of deuterium. The high lamp intensity at this wavenumber results in a saturation of the absorption.

The inhomogeneous broadening effects such as the presence of different site isomers of PTCDA or matrix defects hamper a precise assignment of the spectral features and their substructures. The depositing of PTCDA at the surface of rare gas matrices would decrease inhomogeneous broadening effects. However, in the present case this is not achievable for technical reasons. As an alternative, a beam of large neon clusters is used. After the formation of the clusters, single PTCDA molecules are attached. If the clusters are and, upon doping, remain solid, the chromophore is expected to reside on the cluster surface and hence neon clusters provide a weaker interacting environment (smaller spectral shift and broadening) compared to bulk matrix isolation. On the contrary, if neon clusters are liquid-like, the chromophore is expected to immerse, resulting in similar conformations as in bulk matrices and therefore leading to a similar spectral response. The excitation spectrum obtained for PTCDA-doped neon clusters is displayed in Fig. 4(b), and compared to the absorption spectrum in a Ne matrix (a) and the excitation spectrum in helium droplets (c). An evident correspondence between the neon cluster spectrum and the helium droplet spectrum is observed: the LIF spectrum of PTCDA-doped neon clusters shows the same vibrational modes as observed in helium droplets. The cluster spectrum is broadened and shifted to the red by about  $190\text{ cm}^{-1}$  when compared to the helium droplet spectrum. The neon matrix absorption spectrum is red-shifted by about  $300\text{ cm}^{-1}$  and its main bands as well as the main subfeatures,

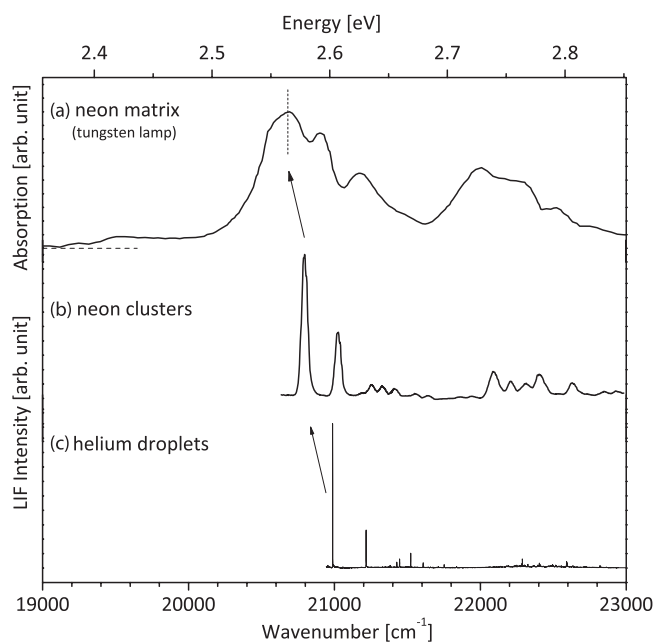


FIG. 4. Absorption spectrum of PTCDA in neon matrix measured with a tungsten halogen lamp (a), compared to the LIF excitation spectrum of PTCDA molecules attached to large neon clusters,  $N = 6000$  (b) or embedded in helium droplets (c).

although much broader, can be clearly assigned to those of the cluster spectrum. The neon matrix is grown slowly at elevated temperatures leading to rather large grain sizes of the polycrystalline solid which is reflected in an enhanced optical transmission. Embedding molecules inside a Ne cluster one would expect a very similar environment as in the matrix case. The apparent differences, however, clearly point to the fact that PTCDA remains on the surface of the clusters which are solid for such sizes ( $N = 6000$ ). The quantitative agreement of vibrational modes will be discussed in Sec. III B.

## B. PTCDA attached to large argon, neon, and para-hydrogen clusters

### 1. Assignment of LIF absorption spectra

Figures 5(a)–5(c) compares the excitation spectra of single PTCDA molecules attached to large argon, para-hydrogen, and neon clusters, to spectra of molecules attached to helium nanodroplets (Fig. 5(d)). In all three cases, vibronic bands are observed even though the resolution is 1–2 orders of magnitude poorer. The argon cluster spectrum of PTCDA is shifted to the red by  $775\text{ cm}^{-1}$  compared to the one obtained in helium droplets. All vibronic bands observed have an identical FWHM of about  $80\text{ cm}^{-1}$ . The overall structure of the spectrum is similar to the one measured in helium droplets, no new lines are observed and the relative positions of the vibronic bands are identical in both cases.

The same observations hold for para-hydrogen and neon clusters. However, due to the weaker interaction, redshifting and broadening are slightly reduced:  $602\text{ cm}^{-1}$  shift for para-hydrogen (FWHM =  $62\text{ cm}^{-1}$ ) and  $190\text{ cm}^{-1}$  shift for

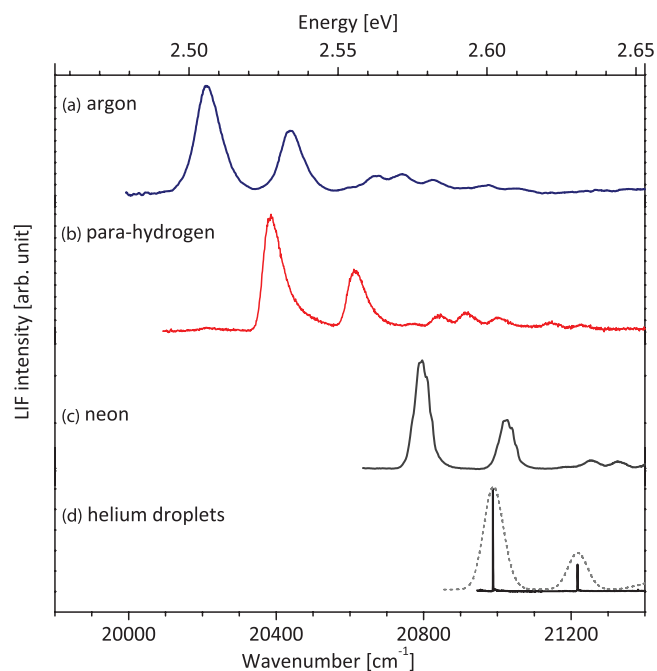


FIG. 5. LIF excitation spectra of PTCDA attached to large argon, para-hydrogen, and neon clusters, compared to the spectra of PTCDA embedded in helium droplets.

neon (FWHM = 47 cm<sup>-1</sup>). If one compares this with the binding energy of the constituents within the cluster: Ar - 450 cm<sup>-1</sup>, H<sub>2</sub> - 50 cm<sup>-1</sup>, and Ne - 120 cm<sup>-1</sup>,<sup>15</sup> one finds that hydrogen, as a molecular and not rare gas constituent, does not follow the order in the amount of the observed shifts. However, when just taking in to account polarizabilities, the larger shift induced by the hydrogen clusters is understandable. In Fig. 6, the shifts are plotted versus atomic/molecular polarizabilities. Although the order is right, we do not find the almost linear dependence, as has been observed before for bulk rare gas matrices and related organic dopants.<sup>60</sup>

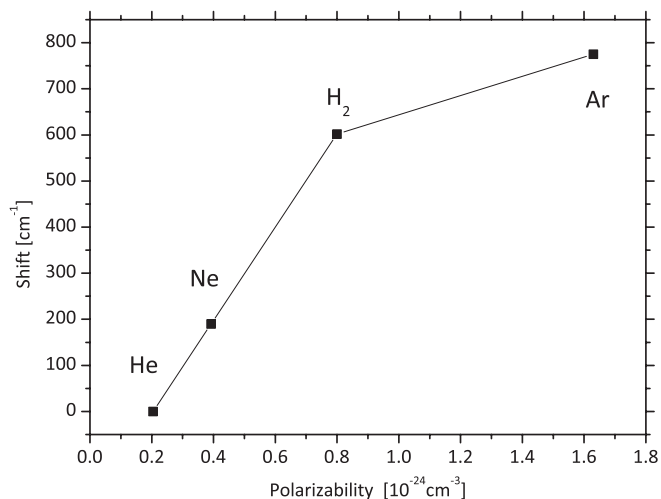


FIG. 6. Shift of lines plotted versus the static polarizabilities of the cluster constituents taken from Ref. 61.

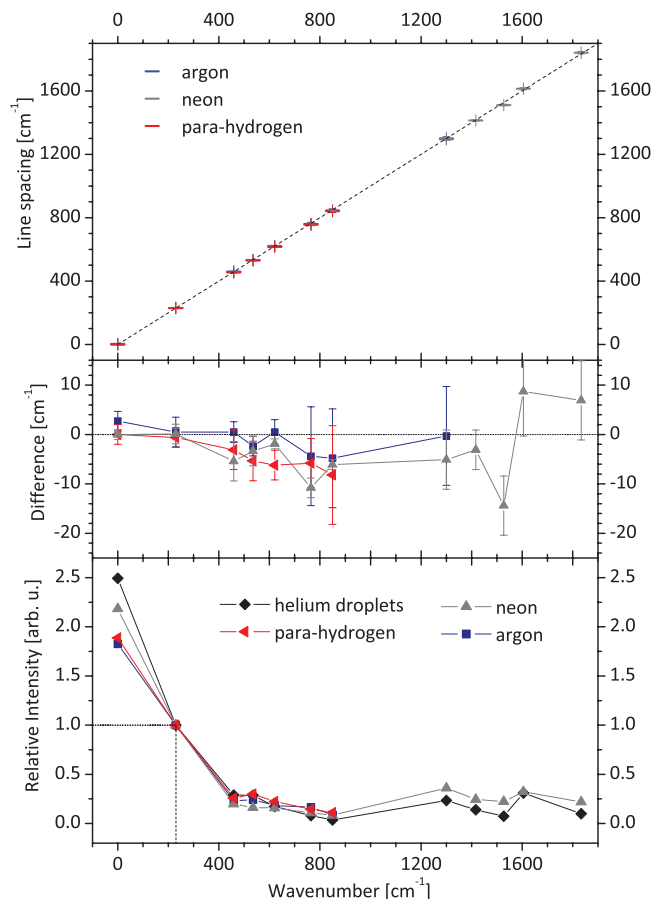


FIG. 7. Extracted vibrational spacings relative to the 0-0 transition of PTCDA-doped argon, neon and para-hydrogen clusters compared to the corresponding lines in helium droplets (top). Difference in absolute numbers (middle). Comparison of relative intensities of the bands (bottom).

The cluster size dependence of the spectra has been studied using different expansion conditions. In the range covered (hundreds to thousands of atoms) no dependence was found meaning that the cluster size does not influence the spectral signature of the chromophore. This implies that the structure of the surface is independent of the cluster size and effects on the curvature of the surface are negligible.

The pick-up of a PTCDA molecule by the host cluster can considerably increase the total energy of the system. We can roughly estimate the energy to be dissipated to about 5000 cm<sup>-1</sup> (3500 cm<sup>-1</sup> collision energy, 500 cm<sup>-1</sup> internal vibrational energy, 1000 cm<sup>-1</sup> formation of rare gas PTCDA bonds, estimated from individual atoms bound to the aromatic rings<sup>62</sup>). This is considerable larger than the sublimation energy of argon clusters of this size (660 cm<sup>-1</sup>) and leads to evaporative cooling. Depending on the redistribution of energy and its dynamics, temporary, local melting cannot be excluded.<sup>63</sup>

Figure 7 (top) plots the relative position of each vibronic band measured in PTCDA-doped rare gas and hydrogen clusters with respect to the corresponding lines observed in helium droplets. The difference shown in absolute numbers (middle) does not point to a significant systematic change of the vibrational spacings when having the PTCDA molecule in the different environments. The relative intensities of the

TABLE I. Peak positions and associated vibrational intervals for the  $S_1 \rightarrow S_0$  transition of PTCDA molecules attached to large argon, neon, and para-hydrogen clusters compared to helium droplets data.

Rare gas and para-H <sub>2</sub> clusters						Helium droplets <sup>54</sup>
Argon		Neon		Para-H <sub>2</sub>		
$\nu$ (cm <sup>-1</sup> )	$\Delta\nu$ (cm <sup>-1</sup> )	$\nu$ (cm <sup>-1</sup> )	$\Delta\nu$ (cm <sup>-1</sup> )	$\nu$ (cm <sup>-1</sup> )	$\Delta\nu$ (cm <sup>-1</sup> )	$\Delta\nu$ (cm <sup>-1</sup> )
20212	0	20797.5	0	20386.4	0	0
20439	227	21027	229.5	20615	229	229.5
20672	460	21251	453.5	20842	456	459
20743	531	21329	532	20916	530	535.25
20827	615	21416	619	21001	615	620.8
20973	761	21551	753.5	21145	759	764.4
...	...	21641	844	21228	842	849.8
21511	1299	22093	1295.5	...	...	1300.3
...	...	22211	1413.5	...	...	1417
...	...	22308	1510.5	...	...	1532.2
...	...	22411	1614	...	...	1603.5
...	...	22638	1840.5	...	...	1832.6

main vibronic lines are presented in Fig. 7 (bottom). As all the peaks of a given spectrum show identical shape and width, the maximal peak intensities can be used for comparisons. The first vibrational mode (at about 230 cm<sup>-1</sup>) has been used for normalization because this mode is less prone to saturation than the 0-0 transition. The relative intensities follow an identical pattern for all the measured spectra. Only weak discrepancies concerning the 0-0 line are observed, attributed to saturation effects. Table I summarizes the extracted line positions. Only weak discrepancies concerning the 0-0 line are observed, attributed to saturation effects. Table I summarizes the extracted line positions.

Measurement in argon matrices could not be achieved successfully. Argon matrices are known to be polycrystalline with much smaller grain sizes than neon leading to a stronger dispersion of the light.<sup>64</sup> In the present spectroscopic configuration the matrix is opaque. With the present experimental setup, the study of para-hydrogen matrix is also not possible. Nevertheless, the analogy of the measurements in neon allow to draw conclusions for argon and para-hydrogen as well.

As outlined in the Introduction, for the cluster sizes considered in the present work, neon, argon, and para-hydrogen clusters are solid. As discussed before, in the case of neon the pronounced difference between the matrix absorption spectrum and the cluster LIF excitation spectrum clearly demonstrates that the PTCDA molecule resides on the surface of solid neon clusters. Moreover, for argon and hydrogen clusters one also observes a similar behavior of broadening and shifting of lines. The relative positions of vibronic bands are identical to the values measured in helium droplets. If the PTCDA molecules were located inside such solid clusters which even have an enhanced interaction, one would clearly expect a much broader and less resolved spectrum. The surface location is further confirmed in recent results on complexes made of a single PTCDA molecule along with argon or para-hydrogen clusters embedded in helium droplets.<sup>65</sup> In that case the use of helium droplets allows for the generation of surface-located but also of embedded PTCDA molecules. The measured spectra clearly show that for both argon and hydrogen a larger shift of embedded molecules occurs. Finally a surface location is also corroborated by previous measurements involving large argon clusters doped with barium or calcium atoms by a pickup process where only surface sites were observed. This was interpreted as proof of the solid phase for such clusters.<sup>66,67</sup> In conclusion our work clearly shows that large rare gas and para-hydrogen clusters made of hundreds to thousands of atoms are solid and doping with PAH molecules results in surface-site occupation only.

## 2. Line broadening and line shape

Besides the redshift, the cluster species has a strong impact on the line broadening as well as the line shape. As for the global spectral shift, these parameters do not show a dependence on the cluster size in the present size range. The shape of the 0-0 transition of PTCDA attached to argon, para-hydrogen and neon clusters is displayed in Fig. 8. We chose to discuss only the 0-0 peaks since the vibrational lines have similar features. Many experiments and theories involving much smaller clusters (up to a few tens of atoms) have

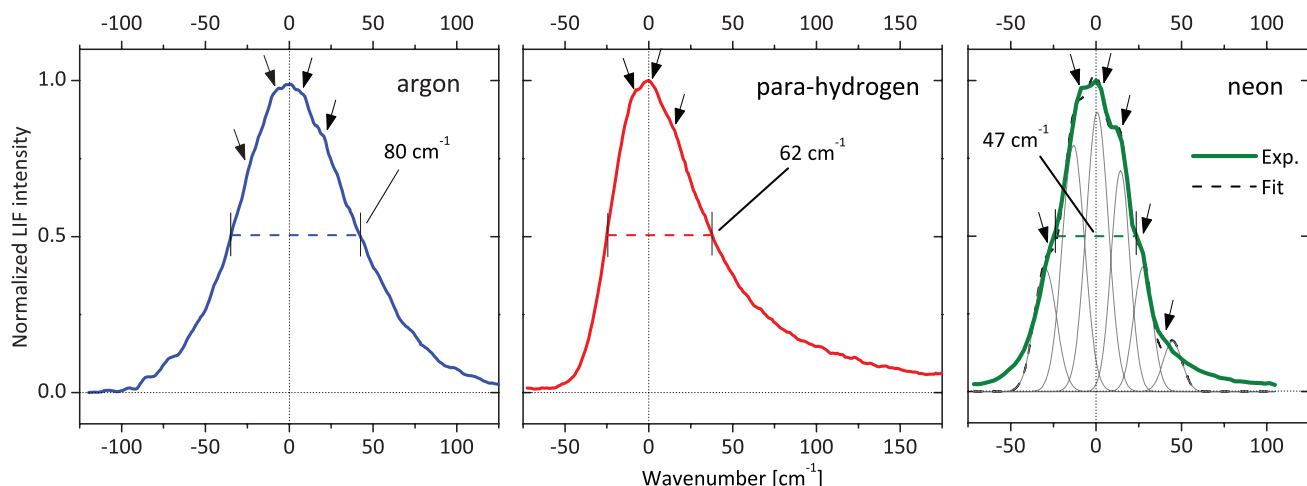


FIG. 8. Line shapes of the  $S_1 \leftarrow S_0$  transition peak of PTCDA molecules attached to argon, para-hydrogen, and neon clusters. Different subfeatures (arrows) are observed which are attributed to different site isomers.

been made in the past, most of which dealing with argon. Tetracene- $\text{Ar}_N$  complexes were shown to have a monotonically increasing linewidth converging for  $N > 20$  atoms to a few tens of  $\text{cm}^{-1}$ .<sup>68</sup> This is interpreted as a manifestation of an inhomogeneous broadening related to the overlap of many coexisting structural isomers which are all homogeneously broadened. Moreover, the clusters' temperature, which is increasing with the cluster size up to some hundreds of atoms,<sup>69</sup> induces some broadening. For example the typical FWHM of the calculated spectrum of tetracene- $\text{Ar}_{26}$  increases from 33 to 72  $\text{cm}^{-1}$  for a cluster temperature rising from 25 to 35 K.<sup>68</sup> In general, the measured lines all show a comparable asymmetry with a more or less pronounced tail extending to the blue. The asymmetry is rather weak for argon and neon but notably stronger when using para-hydrogen clusters.

In the past, calculations have been made on similar systems, perylene- $\text{Ar}_N$  complexes, with the semiclassical spectral density method.<sup>70</sup> This model was developed by Fried *et al.*<sup>71</sup> and takes into account the diffusion of the atoms, the fluctuation of the bond length and electronic energy gap, and the fluctuations of the solvent as well as the cluster asymmetry. The asymmetry is incorporated by introducing a thermal correction factor developed by Islampour *et al.*<sup>72</sup> in their study of the spectral lineshape of molecule doped rigid and non-rigid clusters. Applied to perylene- or benzene-argon complexes this method proved to satisfactorily reproduce experimental measurements and also explain the observed asymmetry toward higher energy of the electronic transitions of the chromophore. However, the calculated FWHM strongly decreases with decreasing temperature and for temperatures below 20 K is smaller than found in the present measurements. One reason might be the much smaller cluster sizes considered. For very small calculated clusters ( $N < 5$ ), isomers having different shifts appear as separated lines. In the present work, substructures are observed (designated by arrows in Fig. 8) and their presence and position are again independent of the cluster size or any other external parameters (laser intensity, doping parameters, etc.). In the spectra presented in Fig. 8, these subfeatures are particularly visible for neon clusters. The presence of such subfeatures clearly hints to inhomogeneous broadening due to different chromophore-cluster conformations (the so-called site-isomers). In the case of neon clusters, the six different subfeatures are fitted with six Gaussian distributions (all of them having here an identical FWHM of about 12  $\text{cm}^{-1}$ ), shifted one to each other. Such an interpretation of a discrete number of isomers having specific spectra can only be true when having well-defined geometric structures (FCC, icosahedral) which again confirms the solid nature of the studied clusters. It would also mean that the deposited molecule anneal to a well defined number of site isomers.

### 3. Formation of dimers and complexes

The overall intensity of the fluorescence signal of PTCDA attached to argon, neon, and para-hydrogen clusters is distinctly higher than for helium droplets (4-5 times for neon clusters). Several reasons can in principle contribute

to that. One could, e.g., have a higher cluster density in the case of argon, neon or para-hydrogen clusters compared to helium droplets. On the other hand, these large solid clusters are able to capture more than one PTCDA molecule. However this does not result in the formation of PTCDA dimers or oligomers and the spectroscopic identity is conserved. In this way multiple absorbers per cluster are provided which results in a higher total signal intensity. In helium droplets the multiple doping of PTCDA gives rise to the formation of oligomers, whose spectral signature is notably different from that of the monomer.

The number of picked-up molecules can be determined when studying the pickup statistics dependent on the density of molecules in the doping cell. For clusters as well as for droplets, the pick-up process is governed by a Poissonian statistics.<sup>73</sup> If one neglects the shrinking of the clusters upon the doping and therefore a reduced capture cross section, the probability  $P(N)$  to collect  $N$  particles after crossing the pick up volume can be written as

$$P(N) = \frac{z^N}{N!} e^{-z}, \quad (1)$$

where  $z$  is the mean number of doping particles picked up by each cluster. This parameter is proportional to the partial pressure of the doping particle in the oven  $p_{dop}$  and is given as follows:

$$z = \frac{\sigma_{cap} L}{k_B T} \sqrt{\frac{\langle v_{clus}^2 \rangle + \langle v_{dop}^2 \rangle}{\langle v_{clus}^2 \rangle}} p_{dop}, \quad (2)$$

where  $L$  is the length of the pickup region,  $\sigma_{cap}$  the capture cross section of the cluster which we assume to be proportional to  $n_0^{2/3}$ ,  $n_0$  being the mean cluster size.  $\langle v_{clus}^2 \rangle$ , and  $\langle v_{dop}^2 \rangle$  are the mean square velocities of the clusters and  $T$  the temperature of the doping cell. A careful study of the Poissonian distribution for low densities in the doping cell gives valuable information on the doping process and allows the distinction between measured signals coming from a single pickup (linear slope), the pickup of two molecules (quadratic slope) or multiple doping (higher polynomial slopes).

When recording LIF intensity as a function of the partial pressure of the doping particle in the oven one can assign the contributions of multiple doped clusters to the spectrum. In Fig. 9, the intensity of the 0-0 line of PTCDA monomer attached to helium droplets or argon, neon, or para-hydrogen clusters are displayed as a function of the PTCDA partial pressure in the oven. The maxima of these distributions are reached at higher temperatures for hydrogen, neon (both at  $\sim 375$  °C), and argon clusters ( $\sim 400$  °C) than for helium droplets ( $\sim 355$  °C). Having higher intensities of monomer absorptions at higher doping levels intuitively indicates that signals come from multiple doped clusters. However, since the position of the maximum is dependent on the pickup cross section, there is some dependence on the cluster size used in the experiment and on a possible different sticking coefficient. In the present case the argon, neon, and para-hydrogen clusters have a mean size of 450, 6000, and 14 000 atoms/molecules, respectively. Using general geometric considerations applied to a FCC packing for these clusters, one



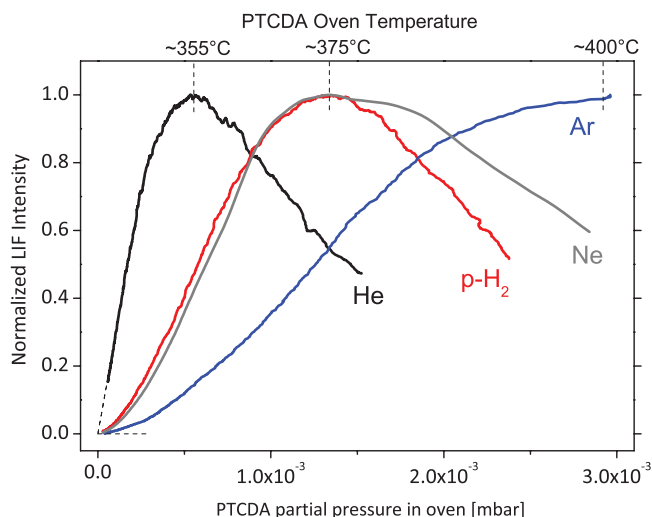


FIG. 9. LIF intensity of the  $S_1 \leftarrow S_0$  transition of PTCDA molecules attached to helium droplets, argon, neon, and para-hydrogen clusters as a function of the PTCDA partial pressure in the oven.

obtains mean values for the cluster diameter of about 60 Å, 125 Å, and 200 Å, respectively. For comparison, the helium droplets have a mean size of roughly 20 000 atoms which corresponds to a diameter of about 100 Å. From these numbers, one would not expect all the maxima lying beyond the position of the maximum of helium droplets. This means that we have multiple absorbers at the clusters that stay immobilized and cannot enter the energetically favorable bound oligomer complex which would alter the optical response. The mobility of the PTCDA molecules on the cluster surface must be strongly quenched which is in contradiction to previous measurements involving smaller chromophores. It has been shown that barium atoms can move freely on argon clusters to form dimers and that such clusters can work successfully as reaction centers for chemical reactions.<sup>20,74</sup> Our results clearly show that this apparently does not apply for larger PAH molecules such as PTCDA where the binding energy is presumably much larger.

Furthermore, an interesting observation is that for hydrogen, neon, and argon, the onset of the curves is not linear, as expected for independent  $z$  absorbers, but dominated by a quadratic dependence on  $z$ . From simulations on the pick-up curves including effects of size distributions, droplet shrinking, momentum, and energy transfer, we can safely exclude experimental effects generating a dependence proportional to  $z^k$ ,  $k > 1$ .<sup>73</sup> We assign this effect to super radiance which gives a quadratic dependence for all oligomer sizes.<sup>75</sup> In a recent publication this effect has been observed at 12 nm separated aromatic chromophores.<sup>76</sup> Since our clusters have diameters below 10 nm, a coherent collective effect should occur as well. This effect will be further analyzed with more detailed studies in the future.

#### IV. CONCLUSION

We present the excitation spectra of PTCDA attached to large argon, neon, and para-hydrogen clusters made of thousands of atoms/molecules. LIF excitation spectra are com-

pared to absorption spectra in solid Ne matrices. The similarity of these spectra to spectra obtained in helium droplets allows the assignment of vibrational modes of PTCDA molecules. The comparison of the excitation spectra with the absorption spectrum of PTCDA in a neon matrix as well as the presence of substructures in the spectral lines prove that only surface sites are occupied by PTCDA and that the cluster surface is solid. Moreover, the precise characterization of the doping process of these clusters points out that the mobility of the chromophore on the cluster surface is strongly suppressed, preventing the formation of PTCDA dimers or oligomers, in contradiction to previous measurements where atoms and smaller molecules were used.

#### ACKNOWLEDGMENTS

Fruitful discussions with Takamasa Momose and Andrey Vilesov are gratefully acknowledged.

- <sup>1</sup>B. W. van de Waal, G. Torchet, and M. F. de Feraudy, *Chem. Phys. Lett.* **331**, 57 (2000).
- <sup>2</sup>B. W. van de Waal, *J. Chem. Phys.* **98**, 4909 (1993).
- <sup>3</sup>S. Kakar, O. Björneholm, J. Weigelt, A. R. B. de Castro, L. Tröger, R. Frahm, T. Möller, A. Knop, and E. Rühl, *Phys. Rev. Lett.* **78**, 1675 (1997).
- <sup>4</sup>M. Y. Hahn and R. L. Whetten, *Phys. Rev. Lett.* **61**, 1190 (1988).
- <sup>5</sup>S. Kakar, O. Björneholm, J. Löfken, F. Federmann, A. V. Soldatov, and T. Möller, *Z. Phys. D* **40**, 84 (1997).
- <sup>6</sup>R. von Pietrowski, M. Rutzen, K. von Haeften, S. Kakar, and T. Möller, *Z. Phys. D* **40**, 22 (1997).
- <sup>7</sup>T. E. Gough, M. Mengel, P. A. Rowntree, and G. Scoles, *J. Chem. Phys.* **83**, 4958 (1985).
- <sup>8</sup>J. Jortner, *Z. Phys. D* **24**, 247 (1992).
- <sup>9</sup>M. Hartmann, R. E. Miller, J. P. Toennies, and A. Vilesov, *Phys. Rev. Lett.* **75**, 1566 (1995).
- <sup>10</sup>S. Leutwyler and J. Bösiger, *Chem. Rev.* **90**, 489 (1990).
- <sup>11</sup>E. L. Knuth, F. Schünemann, and J. P. Toennies, *J. Chem. Phys.* **102**, 6258 (1995).
- <sup>12</sup>S. A. Khairallah, M. B. Sevryuk, D. M. Ceperley, and J. P. Toennies, *Phys. Rev. Lett.* **98**, 183401 (2007).
- <sup>13</sup>K. Kuyanov-Prozument and A. F. Vilesov, *Phys. Rev. Lett.* **101**, 205301 (2008).
- <sup>14</sup>S. Kuma, H. Goto, M. N. Slipchenko, A. Vilesov, A. Khranov, and T. Momose, *J. Chem. Phys.* **127**, 214301 (2007).
- <sup>15</sup>S. Kuma, H. Nakahara, M. Tsubouchi, A. Takahashi, M. Mustafa, G. Sim, T. Momose, and A. F. Vilesov, *J. Phys. Chem. A* **115**, 7392 (2011).
- <sup>16</sup>J. M. Mestdagh, A. J. Bell, J. Berlande, X. Biquard, M. A. Gaveau, A. Lallement, O. Sublemontier, and J. P. Visticot, *Reactions Dynamics in Clusters and Condensed Phases*, edited by J. Jortner, R. D. Levine, and B. Pullman, Vol. 26 of *The Jerusalem Symposium on Quantum Chemistry and Biochemistry* (Kluwer, Dordrecht, 1994).
- <sup>17</sup>X. J. Gu, D. J. Levandier, B. Zhang, G. Scoles, and D. Zhuang, *J. Chem. Phys.* **93**, 4898 (1990).
- <sup>18</sup>X. Biquard, O. Sublemontier, J. Berlande, M. A. Gaveau, J. M. Mestdagh, and J. P. Visticot, *J. Chem. Phys.* **103**, 957 (1995).
- <sup>19</sup>A. Lallement, J. Cuvellier, J. M. Mestdagh, P. Meynadier, P. de Pujo, O. Sublemontier, J. P. Visticot, J. Berlande, and X. Biquard, *Chem. Phys. Lett.* **189**, 182 (1992).
- <sup>20</sup>A. Lallement, O. Sublemontier, J. P. Visticot, A. J. Bell, J. Berlande, J. Cuvellier, J. M. Mestdagh, and P. Meynadier, *Chem. Phys. Lett.* **204**, 440 (1993).
- <sup>21</sup>A. Leger and J. L. Puget, *Astron. Astrophys.* **137**, L5 (1984).
- <sup>22</sup>F. Salama, C. Joblin, and L. J. Allamandola, *Planet. Space Sci.* **43**, 1165 (1995).
- <sup>23</sup>Q. H. Wang and M. C. Hersam, *Nat. Chem.* **1**, 206 (2009).
- <sup>24</sup>H. Proehl, R. Nitsche, T. Diemel, K. Leo, and T. Fritz, *Phys. Rev. B* **71**, 165207 (2005).
- <sup>25</sup>F. Schreiber, *Prog. Surf. Sci.* **65**, 151 (2000).
- <sup>26</sup>S. R. Forrest, *Chem. Rev.* **97**, 1793 (1997).

- <sup>27</sup>M. Müller, A. Langner, O. Krylova, E. L. Moal, and M. Sokolowski, *Appl. Phys. B* **105**, 67 (2011).
- <sup>28</sup>M. H. Hennessey, Z. G. Soos, R. A. Pascal, and A. Girlando, *Chem. Phys.* **245**, 199 (1999).
- <sup>29</sup>P. Peumans, A. Yakimov, and S. R. Forrest, *J. Appl. Phys.* **93**, 3693 (2003).
- <sup>30</sup>A. W. Hains, Z. Liang, M. A. Woodhouse, and B. A. Gregg, *Chem. Rev.* **110**, 6689 (2010).
- <sup>31</sup>R. R. Lunt, J. B. Benziger, and S. R. Forrest, *Adv. Mater.* **22**, 1233 (2010).
- <sup>32</sup>M. E. Jacox, *J. Phys. Chem. Ref. Data* **32**, 1 (2003).
- <sup>33</sup>A. Sassara, G. Zerza, and M. Chergui, *J. Phys. B* **29**, 4997 (1996).
- <sup>34</sup>F. Salama and L. J. Allamandola, *J. Chem. Phys.* **94**, 6964 (1991).
- <sup>35</sup>F. Salama, C. Joblin, and L. J. Allamandola, *J. Chem. Phys.* **101**, 10252 (1994).
- <sup>36</sup>T. M. Halasinski, D. M. Hudgins, F. Salama, L. J. Allamandola, and T. Bally, *J. Phys. Chem. A* **104**, 7484 (2000).
- <sup>37</sup>C. Crépin and A. Tramer, *Chem. Phys. Lett.* **170**, 446 (1990).
- <sup>38</sup>X. Chillier, P. Boulet, H. Chermette, F. Salama, and J. Weber, *J. Chem. Phys.* **115**, 1769 (2001).
- <sup>39</sup>C. Joblin, F. Salama, and L. Allamandola, *J. Chem. Phys.* **102**, 9743 (1995).
- <sup>40</sup>C. Joblin, F. Salama, and L. Allamandola, *J. Chem. Phys.* **110**, 7287 (1999).
- <sup>41</sup>E. Engel, K. Schmidt, D. Beljonne, J.-L. Brédas, J. Assa, H. Fröb, K. Leo, and M. Hoffmann, *Phys. Rev. B* **73**, 245216 (2006).
- <sup>42</sup>M. Dvorak, M. Müller, T. Knoblauch, O. Bünermann, A. Rydlo, S. Minnerberger, W. Harbich, and F. Stienkemeier, *J. Chem. Phys.* **137**, 164302 (2012).
- <sup>43</sup>F. Conus, J. T. Lau, V. Rodrigues, and C. Felix, *Rev. Sci. Instrum.* **77**, 113103 (2006).
- <sup>44</sup>E. Ilisca, *Prog. Surf. Sci.* **41**, 217 (1992).
- <sup>45</sup>P. Rock, *Chemical Thermodynamics* (MacMillan, 1969).
- <sup>46</sup>O. F. Hagena and W. Obert, *J. Chem. Phys.* **56**, 1793 (1972).
- <sup>47</sup>J. Cuvelier, P. Meynadier, P. de Pujo, O. Sublemontier, J.-P. Visticot, J. Berlande, A. Lallement, and J.-M. Mestdagh, *Z. Phys. D* **21**, 265 (1991).
- <sup>48</sup>M. A. Gaveau, M. Briant, P. R. Fournier, J. M. Mestdagh, and J. P. Visticot, *Phys. Chem. Chem. Phys.* **2**, 831 (2000).
- <sup>49</sup>W. Obert, *Rarefied Gas Dyn.* **2**, 1181 (1979).
- <sup>50</sup>E. Knuth, S. Schaper, and J. P. Toennies, *J. Chem. Phys.* **120**, 235 (2004).
- <sup>51</sup>J. Harms, J. P. Toennies, and F. Dalfovo, *Phys. Rev. B* **58**, 3341 (1998).
- <sup>52</sup>J. Farges, M.-F. de Feraudy, B. Raoult, and G. Torchet, *Surf. Sci.* **106**, 95 (1981).
- <sup>53</sup>J. P. Toennies and A. F. Vilesov, *Angew. Chem., Int. Ed.* **43**, 2622 (2004).
- <sup>54</sup>M. Wewer and F. Stienkemeier, *J. Chem. Phys.* **120**, 1239 (2004).
- <sup>55</sup>M. Wewer, Ph.D. dissertation, Universität Bielefeld, 2004.
- <sup>56</sup>N. Karl and N. Sato, *Mol. Cryst. Liq. Cryst.* **218**, 79 (1992).
- <sup>57</sup>Y. Hirose, W. Chen, E. I. Haskal, S. R. Forrest, and A. Kahn, *Appl. Phys. Lett.* **64**, 3482 (1994).
- <sup>58</sup>I. G. Hill, A. Rajagopal, A. Kahn, and Y. Hu, *Appl. Phys. Lett.* **73**, 662 (1998).
- <sup>59</sup>T. M. Halasinski, J. L. Weisman, R. Ruiterkamp, T. J. Lee, F. Salama, and M. Head-Gordon, *J. Phys. Chem. A* **107**, 3660 (2003).
- <sup>60</sup>I. Biktchantaev, V. Samartsev, and J. Sepiol, *J. Lumin.* **98**, 265 (2002).
- <sup>61</sup>D. Lide, *CRC Handbook of Chemistry and Physics: A Ready-Reference Book of Chemical and Physical Data* (CRC, 2006).
- <sup>62</sup>N. Pörtner, A. F. Vilesov, and M. Havenith, *Chem. Phys. Lett.* **343**, 281 (2001).
- <sup>63</sup>A. V. Malakhovskii and M. Ben-Zion, *Chem. Phys.* **264**, 135 (2001).
- <sup>64</sup>M. Klein and J. Venables, *Rare Gas Solids* (Academic, 1976).
- <sup>65</sup>M. Dvorak, O. Bünermann, and F. Stienkemeier, "Phase state of hydrogen and argon clusters attached to PTCDA-doped helium nanodroplets," (unpublished).
- <sup>66</sup>J. P. Visticot, P. de Pujo, J. M. Mestdagh, A. Lallement, J. Berlande, O. Sublemontier, P. Meynadier, and J. Cuvelier, *J. Chem. Phys.* **100**, 158 (1994).
- <sup>67</sup>M. A. Gaveau, M. Briant, P. R. Fournier, J. M. Mestdagh, J. P. Visticot, F. Calvo, S. Baudrand, and F. Spiegelman, *Eur. Phys. J. D* **21**, 153 (2002).
- <sup>68</sup>N. Ben-Horin, U. Even, J. Jortner, and S. Leutwyler, *J. Chem. Phys.* **97**, 5296 (1992).
- <sup>69</sup>A. Rytönen, S. Valkealahti, and M. Manninen, *J. Chem. Phys.* **108**, 5826 (1998).
- <sup>70</sup>A. Heidenreich and J. Jortner, *Z. Phys. D* **26**, 377 (1993).
- <sup>71</sup>L. E. Fried and S. Mukamel, *J. Chem. Phys.* **96**, 116 (1992).
- <sup>72</sup>R. Islampour and S. Mukamel, *Chem. Phys. Lett.* **107**, 239 (1984).
- <sup>73</sup>O. Bünermann and F. Stienkemeier, *Eur. Phys. J. D* **61**, 645 (2011).
- <sup>74</sup>X. Biquard, O. Sublemontier, J. P. Visticot, J. M. Mestdagh, P. Meynadier, M. A. Gaveau, and J. Berlande, *Z. Phys. D* **30**, 45 (1994).
- <sup>75</sup>N. E. Rehler and J. H. Eberly, *Phys. Rev. A* **3**, 1735 (1971).
- <sup>76</sup>C. Hettich, C. Schmitt, J. Zitzmann, S. Kühn, I. Gerhardt, and V. Sandoghdar, *Science* **298**, 385 (2002).